Paper No. 85. (quote when citing this article)
Eleventh World Conference on Earthquake Engineering
ISBN: 0 08 042822 3

A SIMPLIFIED SEISMIC RESPONSE ANALYSIS OF AN EMBEDDED CYLINDRICAL STRUCTURE

Y. SHIMOMURA[1] and Y. IKEDA[2]

[1]Department of Construction, Junior College of Nihon University,
7-24-1 Narashino-dai, Funabashi-City, Chiba 274 Japan

[2]Nuclear Facilities Department, Taisei Corporation,
1-25-1 Nishi Shinjuku, Shinjuku-ku, Tokyo 163-06 Japan

ABSTRACT

This paper proposes a simplified analytical method for computing the dynamic soil stiffness for a cylindrical structure embedded in a finite soil stratum supported by a rock half-space. For a whole side surface of the embedded structure, an averaged horizontal soil stiffness that can consider a resonance effect of the finite stratum and a confining effect of impedance ratio of the rock half-space to the finite soil stratum is derived. The validity of the proposed method is examined by comparing it to results of the 3-dimensional thin layer approach. Results of the proposed method show a good agreement with those of the 3-dimensional analysis.

KEYWORDS

Embedded structure; half-space support; Novak's soil spring; practical analysis; resonance of finite soil stratum; sway-rocking (SR) model; thin layer approach.

INTRODUCTION

Analyzing dynamic response of embedded structures, especially to estimate side soil stiffnesses for the structures, dynamic soil springs based on an assumption of Winkler type foundation have been well known and utilized for their convenience and relevance (Novak *et al.*, 1978) . Because of the limitation of such assumption, it is difficult for those springs to represent 3-dimensional soil behaviors and a resonance effect of a finite soil stratum supported by a rock half-space. The purpose of this paper is to present an improved analytical method that can take the above effects into account for obtaining an averaged horizontal soil stiffness and demonstrate numerical examples of the averaged horizontal soil stiffnesses for a whole side surface of the embedded structure with impedance ratios of the rock half-space to the finite soil stratum and aspect ratios of the structure. The relevance and accuracy of the proposed method are verified by displacements of rigid structure and moment of the structure due to horizontal subgrade reactions of the surrounding soil. The 3-dimensional thin layer approach referred for derivation of the proposed method has been adopted as an exact solution in this paper (Tajimi *et al.*, 1977).

HORIZONTAL SOIL STIFFNESS SURROUNDING STRUCTURE

Model for Simplified Analysis

First, horizontal motion of the structure embedded in a horizontally homogeneous, elastic surface soil layer (a finite soil stratum) overlying generally a relative hard (a rock half-space) is defined. In this case, an impedance

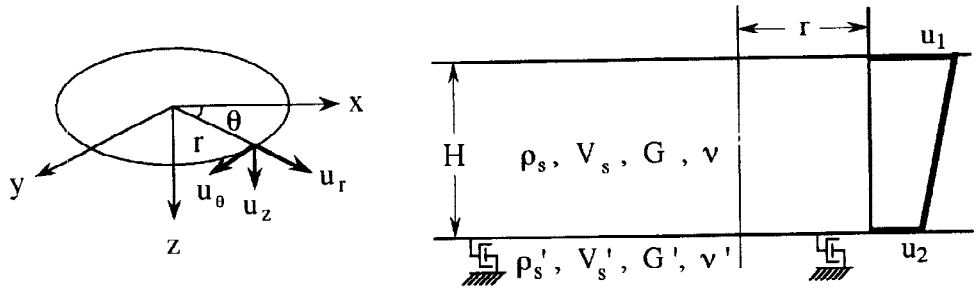

Fig. 1. Analysis model and coordinate system.

for the finite soil stratum is assumed as ρV_S (ρ:mass density; V_S:velocity of S-wave) and that for the rock half-space is presumed as $s\rho V_S$ ($s=\rho' V_S'/\rho V_S$:impedance ratio; superscript(') represents the physical constants of the rock half-space). Fig. 1 illustrates the massless rigid cylindrical foundation embedded in the finite soil stratum mentioned the above, whose radius and depth are r_0 and D, respectively. The total system of the soil shown in Fig. 1 is assumed as a model composed of a single thin layer and a dashpot-mat. The vertical deformation of the soil is omitted and the horizontal deformation is assumed to vary linearly along z-direction. The horizontal displacement vector is thus defined in the form

$$\{u\} = (u_1, u_2)^T \exp(i\omega t) \tag{1}$$

where, i; imaginary number and ω; circular frequency.

Derivation of Soil Stiffness

The general solution of the 3-dimensional wave equation for the thin layer soil model in the cylindrical coordinates gives the following horizontal displacement vectors that are specified at each nodal interface:

$$\{u_r\} = \{v_r\}\cos\theta, \quad \{u_\theta\} = \{v_\theta\}\sin\theta, \tag{2}$$

where,

$$\begin{aligned} \{v_r\} &= \frac{1}{2}[H_2^{(2)}(\alpha r) - H_0^{(2)}(\alpha r)]\{X\} + \frac{1}{2}[H_2^{(2)}(\beta r) + H_0^{(2)}(\beta r)]\{Y\}, \\ \{v_\theta\} &= \frac{1}{2}[H_2^{(2)}(\alpha r) + H_0^{(2)}(\alpha r)]\{X\} + \frac{1}{2}[H_2^{(2)}(\beta r) - H_0^{(2)}(\beta r)]\{Y\}. \end{aligned} \tag{3}$$

$H_\nu^{(2)}(*)$ =Hankel function of the 2nd kind of the n-th order.
In the above, the time function $\exp(i\omega t)$ is omitted. The wave numbers α and β, and the horizontal displacement vectors at each nodal interface {X} and {Y} must satisfy the eigenvalue equations:

$$\begin{aligned} (\beta^2[A_S] + [G_S] - \omega^2[M])\{Y\} &= \{0\}, \\ (\alpha^2[A_p] + [G_S] - \omega^2[M])\{X\} &= \{0\}. \end{aligned} \tag{4}$$

where, $[A_S], \ldots, [M]$ are assemblies of the corresponding element matrix of

$$\begin{aligned} &[A_S] = GH[E_1], \quad [G_S] = \frac{G}{H}[E_2] + i\omega\rho' V_s'[E_3], \quad [A_p] = (\lambda + 2G)H[E_1], \\ &[M] = \rho H[E_1], \quad [E_1] = \frac{1}{6}\begin{bmatrix} 2 & 1 \\ 1 & 2 \end{bmatrix}, \quad [E_2] = \begin{bmatrix} 1 & -1 \\ -1 & 1 \end{bmatrix}, \quad [E_3] = \begin{bmatrix} 0 & 0 \\ 0 & 1 \end{bmatrix}. \end{aligned} \tag{5}$$

Where, G:shear modulus of elasticity, λ:Lame's constant, ρ:mass density of soil, H:thickness of layer, and superscript (') denotes the dashpot-mat properties. Here, consider a single layer of the thickness H and having a hole of radius r_0 at its center, where the top and bottom surfaces are designated by 1 and 2. The solutions of Eq.(4) are

$$\beta_1 = \frac{1}{H}\left[\left(\frac{\omega H}{V_s}\right)^2 - 6\left(1 + f_1(C)\right)\right]^{1/2}, \quad \alpha_1 = \zeta\beta_1, \quad \{X_1\} = \{Y_1\} = \{S_1\},$$
$$\beta_2 = \frac{1}{H}\left[\left(\frac{\omega H}{V_s}\right)^2 - 6\left(1 + f_2(C)\right)\right]^{1/2}, \quad \alpha_2 = \zeta\beta_2, \quad \{X_2\} = \{Y_2\} = \{S_2\}. \tag{6}$$

where, $C = s\omega r/V_S$, $\zeta = V_S/V_p$, V_S:shear wave velocity, V_p:compressive wave velocity and

$$\{S_1\} = (1,\ 1/f_2(C))^T, \quad \{S_2\} = (1,\ 1/f_1(C))^T,$$
$$f_1(z) = iz/3 - f(z), \quad f_2(z) = iz/3 + f(z), \quad f(z) = \sqrt{(1+iz/3)^2 - iz/3}\ . \tag{7}$$

Now, the displacement vectors at the radius r_0 are defined in the form

$$\{U_r\} = \{V_r\}\cos\theta\ , \quad \{U_\theta\} = \{V_\theta\}\sin\theta. \tag{8}$$

Vectors $\{V_r\}$ and $\{V_\theta\}$ can be given from Eq.(3) as follows

$$\{V_r\} = \frac{1}{2}\sum_{j=1}^{2}\left[H_2^{(2)}(\alpha_j r_0) - H_0^{(2)}(\alpha_j r_0)\right]\{X_j\}q_{\alpha_j} + \frac{1}{2}\sum_{j=1}^{2}\left[H_2^{(2)}(\beta_j r_0) + H_0^{(2)}(\beta_j r_0)\right]\{Y_j\}q_{\beta_j},$$
$$\{V_\theta\} = \frac{1}{2}\sum_{j=1}^{2}\left[H_2^{(2)}(\alpha_j r_0) + H_0^{(2)}(\alpha_j r_0)\right]\{X_j\}q_{\alpha_j} + \frac{1}{2}\sum_{j=1}^{2}\left[H_2^{(2)}(\beta_j r_0) - H_0^{(2)}(\beta_j r_0)\right]\{Y_j\}q_{\beta_j}. \tag{9}$$

Now, assuming that a circular rigid plate with radius r_0 is embedded in the hole and subjected to a harmonic sway motion with amplitude $\{V_x\}$ in the x-direction. Then one has

$$\{V_x\} = \{V_r\} = \{V_\theta\}. \tag{10}$$

In general, the relationships between stress and strain in the polar coordinate are indicated in the forms,

$$\sigma_{rr} = -p_r\cos\theta, \quad \sigma_{r\theta} = -p_\theta\sin\theta, \tag{11}$$

where

$$p_r = -\left[\lambda\left\{\frac{1}{r}\frac{\partial}{\partial r}(r v_r) + \frac{v_\theta}{r}\right\} + 2G\frac{\partial v_r}{\partial r}\right]_{r=r_0}, \quad p_\theta = -G\left(\frac{\partial v_\theta}{\partial r} - \frac{v_\theta + v_r}{r}\right)_{r=r_0}. \tag{12}$$

Then x-directional resultant force, $\overline{P}_x$, at a unit depth is given as follow

$$\overline{P}_x = -2\int_{-\pi/2}^{\pi/2}\left(\sigma_{rr}\cos\theta - \sigma_{r\theta}\sin\theta\right) r_0\, d\theta = \pi r_0\left(p_r - p_\theta\right). \tag{13}$$

The total forces P_{xj} (j=1,2) working at the surfaces (1,2) in the x-direction are

$$P_{xj} = \pi r_0\int_{-H/2}^{H/2} N_j\left(p_r - p_\theta\right) dz, \tag{14}$$

where N_j are the interpolation functions and are given by $N_1 = 1/2 - z/H$, $N_2 = 1/2 + z/H$, respectively. Thus, the force vector $\{P_x\} = [P_{x1},\ P_{x2}]^T$ becomes

$$\{P_x\} = \pi GH\left[F(\alpha_1,\beta_1,r_0)\left([E_1] + g(C)[E_4] + h(C)[E_1] - \frac{h(C)}{2}[E_3]\right)\right.$$
$$\left. + F(\alpha_2,\beta_2,r_0)\left([E_1] - g(C)[E_4] - h(C)[E_1] - \frac{h(C)}{2}[E_3]\right)\right]\{V_x\}, \tag{15}$$

where,

$$F(\alpha,\beta,r) = \beta r\frac{H_2^{(2)}(\alpha r)H_1^{(2)}(\beta r) + H_2^{(2)}(\beta r)H_1^{(2)}(\alpha r)/\zeta}{H_2^{(2)}(\beta r)H_0^{(2)}(\alpha r) + H_2^{(2)}(\alpha r)H_0^{(2)}(\beta r)},$$
$$g(z) = 1/f(z), \quad h(z) = iz/3\,f(z), \quad [E_4] = \frac{1}{6}\begin{bmatrix}1 & 2\\ 2 & 1\end{bmatrix}. \tag{16}$$

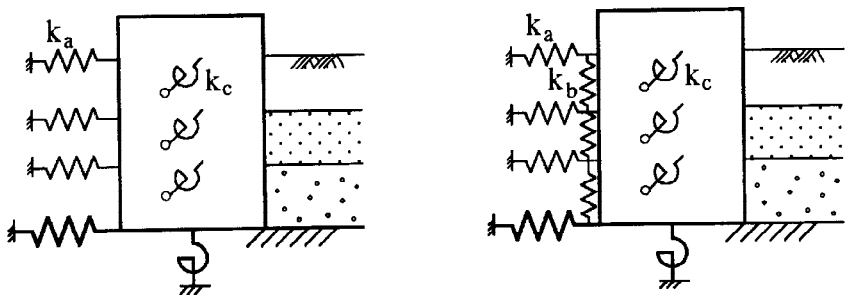

(a) Model without shear spring k_b (b) Model with shear spring k_b

Fig. 2. Soil spring model for an embedded structure.

DISCRETE SOIL SPRING MODEL

In general, structures and soils are modeled by masses and springs, and dynamic soil stiffnesses in SR-model. The dynamic soil stiffnesses for SR-model are typically assumed to be composed of contributions of side and bottom soil stiffnesses of an embedded structure as shown in Fig.2. Especially, the side soil stiffness consists of two components, that is, laterally axial stiffness, k_a and rotational stiffness, k_c. Both dynamic stiffnesses have been well known as Novak's springs. The model using Novak's springs is quite convenient and applicable for the embedded structures, on the other hand, it has difficulty in representing 3-dimensional soil behaviors. Focusing on this point, an improved soil model added shear stiffness, k_b that can counterbalance with the above soil characteristics has been proposed. For cases of impedance ratio s=0 and s=∞, a procedure to obtain the shear stiffness with laterally axial stiffness independent of impedance ratio has been also presented (Ikeda *et al.*, 1992, Shimomura *et al.*, 1995). In this section, an approach to estimate laterally axial and shear stiffnesses dependent on impedance ratio is proposed using the derivation in the previous section.

Assuming that the laterally axial stiffness k_a varies along z-direction, Eq.(15) can be rewritten as follow,

$$\{P_x\} = [K]\{V_x\}. \tag{17}$$

where, stiffness matrix [K] is given as

$$[K] = \begin{bmatrix} K_{11} & K_{12} \\ K_{21} & K_{22} \end{bmatrix} = \frac{H}{12}\begin{bmatrix} 3\tilde{k}_{a1}+\tilde{k}_{a2} & \tilde{k}_{a1}+\tilde{k}_{a2} \\ \tilde{k}_{a1}+\tilde{k}_{a2} & \tilde{k}_{a1}+3\tilde{k}_{a2} \end{bmatrix} + k'\begin{bmatrix} 1 & -1 \\ -1 & 1 \end{bmatrix}. \tag{18}$$

Now, the laterally axial stiffness for a unit depth $\tilde{k}_{a1}$, $\tilde{k}_{a2}$ designated at the top and bottom surface and stiffness k' can be represented as followings,

$$\tilde{k}_{a1} = \pi G[\{1+g(C)+2h(C)\}F(\alpha_1,\beta_1,r_0) + \{1-g(C)-2h(C)\}F(\alpha_2,\beta_2,r_0)], \tag{19}$$

$$\tilde{k}_{a2} = \pi G[\{1+g(C)-h(C)\}F(\alpha_1,\beta_1,r_0) + \{1-g(C)+h(C)\}F(\alpha_2,\beta_2,r_0)], \tag{20}$$

$$k' = \pi GH[2g(C)+h(C)][F(\alpha_2,\beta_2,r_0) - F(\alpha_1,\beta_1,r_0)] / 12. \tag{21}$$

Case s→0 In case when s converges at 0, functions of g(C) and h(C) would converge 1 and 0, respectively. So, Eq.(15) yields to the following relationship between the nodal force vector and displacement one,

$$\{P_x\} = \pi GH\left(\frac{F(\bar{\alpha}_1,\bar{\beta}_1,r_0)}{2}\begin{bmatrix} 1 & 1 \\ 1 & 1 \end{bmatrix} + \frac{F(\bar{\alpha}_2,\bar{\beta}_2,r_0)}{6}\begin{bmatrix} 1 & -1 \\ -1 & 1 \end{bmatrix}\right)\{V_x\}, \tag{22}$$

where

$$\bar{\beta}_1 = \frac{\omega}{V_s},\quad \bar{\beta}_2 = -i\frac{1}{H}\sqrt{12-\left(\frac{\omega H}{V_s}\right)^2},\quad \bar{\alpha}_j = \zeta\bar{\beta}_j. \tag{23}$$

Eq.(23) coincides with our previous result for a unit thin layer without support (Ikeda *et al.*, 1992). In this case, the laterally axial stiffness $\tilde{k}_{a1}$ for the top nodal surface is identical with $\tilde{k}_{a2}$ for the bottom one, so the constant laterally axial stiffness for a unit depth $\tilde{k}_a$ is given as

$$\tilde{k}_a = 2\pi G\, F(\bar{\alpha}_1, \bar{\beta}_1, r_0)\,. \tag{24}$$

Eq.(24) coincides with the Novak's result and the shear stiffness k_b is written as (Novak *et al.*, 1978),

$$k_b = k' - \tilde{k}_a / 12 = \pi GH\,[F(\bar{\alpha}_2, \bar{\beta}_2, r_0) - F(\bar{\alpha}_1, \bar{\beta}_1, r_0)] / 6\,. \tag{25}$$

Case $s \to \infty$ In case when s converges at ∞, functions of g(C) and h(C) would become 0 and 1, respectively. So Eq.(15) yields to the following,

$$\{P_x\} = \pi GH \left(\frac{F(\hat{\alpha}_1, \hat{\beta}_1, r_0)}{6}\begin{bmatrix} 4 & 2 \\ 2 & 3 \end{bmatrix} + \frac{F(\hat{\alpha}_2, \hat{\beta}_2, r_0)}{2}\begin{bmatrix} 0 & 0 \\ 0 & 1 \end{bmatrix}\right) \{V_x\}\,. \tag{26}$$

The relationship between the nodal force and displacement at the top surface is written as,

$$P_{x1} = K_{11} V_{x1} = \frac{2\pi GH}{3} F(\hat{\alpha}_1, \hat{\beta}_1, r_0) V_{x1}\,, \tag{27}$$

where,

$$\hat{\beta}_1 = -i\frac{1}{H}\sqrt{3 - \left(\frac{\omega H}{V_s}\right)^2}\,,\quad \hat{\alpha}_1 = \zeta \hat{\beta}_1\,. \tag{28}$$

Eqs.(27) and (28) also coincide with our previous results (Shimomura *et al.*, 1995).

NUMERICAL EXAMPLES AND DISCUSSIONS FOR SOIL STIFFNESSES

Derivation of Averaged Horizontal Soil Stiffness

Derivation of horizontal displacement of the soil along the side surface of the structure is assumed as

$$V(z) = N_1 V_1 + N_2 V_2 = (1/2 - z/H) V_1 + (1/2 + z/H) V_2\,. \tag{29}$$

Now, the averaged soil stiffness is defined as $\bar{k}$. Substituting $V_2 = 0$ into Eq.(29), soil reaction at an arbitrary depth, $\sigma(z)$, is given as

$$\sigma(z) = \bar{k}\, N_1 V_1 = \bar{k}\,(1/2 - z/H) V_1\,. \tag{30}$$

Then, the nodal force at the top surface can be derived by the same manner as Eq.(14)

$$P_1 = \int_{-H/2}^{H/2} N_1\, \sigma(z)\, dz = \bar{k} \int_{-H/2}^{H/2} N_1^2\, V_1\, dz = \frac{\bar{k}}{3} V_1\,. \tag{31}$$

Finally, the averaged soil stiffness can be obtained by Eqs.(15) and (31)

$$\bar{k} = \pi G[\{1 + g(C)/2 + h(C)\}\, F(\alpha_1, \beta_1, r_0) + \{1 - g(C)/2 - h(C)\}\, F(\alpha_2, \beta_2, r_0)]\,. \tag{32}$$

Numerical Results of Averaged Horizontal Soil Stiffness

To confirm the applicability of the proposed method, first, the averaged horizontal stiffnesses due to the horizontal subgrade reactions of the surrounding soil of the embedded rigid structure are estimated. Aspect

ratios of the structure and impedance ratios of a rock half-space to a finite soil stratum are employed as parameters.

Fig.3 shows the averaged horizontal stiffnesses for a unit depth with the impedance ratios, s=1, 2, 5 and 1000 and aspect ratio $r_0/H=1$ where r_0 is the radius of the rigid structure, H is a height of a finite soil stratum. Below the natural frequency of the finite soil stratum (ω_g), the real parts of the stiffnesses increase with increasing of the impedance of the rock half-space (confining effects of the rock half-space). Because the rock half-space is modeled in terms of a dashpot-mat, the real parts of the stiffnesses drop rapidly below the peak frequency. Practically, static stiffnesses can be assumed to be the maximum values of the real parts of the stiffnesses. Furthermore, in the range below the peak frequency, the values of the real parts of the stiffnesses are larger than for the Novak's spring. The imaginary parts of the stiffnesses in the low frequencies increase with decreasing of the impedance of the rock half-space. It means that wave transmits below the dashpot-mat. In cases of low impedance ratios, the proposed method can represent the dissipation of energy transmitted below the dashpot-mat. Above about twice the natural frequency, there is no difference between the proposed stiffnesses and Novak's one, because the surrounding soil would behave as the lateral wave propagation resistance.

Figs. 4 and 5 show the averaged horizontal stiffnesses for a unit depth with aspect ratios, $r_0/H=1/4$, 1/2, 1 and 2, and impedance ratio s=5. The real and imaginary parts of the stiffnesses in Fig.4 are represented by non-dimensional stiffness k/G. On the other hand, Fig.5 has a longitudinal axis of $k/G(r_0/H)^{3/4}$ and $k/G(r_0/H)$ for the real and imaginary parts of the stiffnesses, respectively. Beyond twice the natural frequency of the finite soil stratum, there is no difference with respect to aspect ratios for the real parts of the stiffnesses. The real parts of the stiffnesses in the low frequency range would be proportional to $(r_0/H)^{3/4}$ and the imaginary parts would also be proportional to (r_0/H) in all frequency range.

SEISMIC RESPONSE OF AN EMBEDDED STRUCTURE

Seismic responses of a cylindrical rigid structure embedded in a finite soil stratum sustained by a rigid base are performed in our previous paper (Shimomura *et al.*, 1995). In this paper, the same seismic responses are examined with the soil stiffnesses discussed in the previous section to compare with the responses of the 3-dimensional thin layer approach (TLEM). Fig.6 shows an ideal model of a cylindrical rigid structure in a finite soil stratum supported by a rock half-space.

Numerical Results and Discussions

In the following analyses, it is assumed that the embedded depth of the structure is H(=12m), which is divided into n(=12) sub-layers, impedance ratio of the rock half-space to the finite soil stratum is s(=3), and the radius of the structure is r_0(=H/2). The hysteretic damping of soil is neglected.

Fig.7 shows modulus of amplification from the free field at the free surface to the top of structure and that of non-dimensional coefficients of subgrade reactions. In both cases, it is assumed that Poisson's ratio of soil is ν(=0.4), aspect ratio is r_0/H(=1/2), and the mass ratio of structure to soil is m_b/m_s(=1/2). Those figures include the response by the proposed method, Novak's model and the 3-dimensional thin layer approach. Since the proposed method provides frequencies about 10% higher than for the 3-dimensional results, the natural frequency of the finite soil stratum that generates a valley is also higher than for the 3-dimensional analysis. It is indicated that non-dimensional coefficient of subgrade reactions predicted with the proposed method are in good agreement with for TLEM, especially in the low frequency range.

CONCLUSIONS

A simplified analytical method that can provide the dynamic soil stiffness for the structure embedded in a finite soil stratum supported by a rock half-space was proposed. The averaged stiffness derived from the above stiffness can take not only the resonance effect of the finite soil layer but also the confining effect of impedance ratio of the rock half-space to the finite soil stratum into account. It is also indicated that the averaged stiffness depends on aspect ratios of the structure, r_0/H.

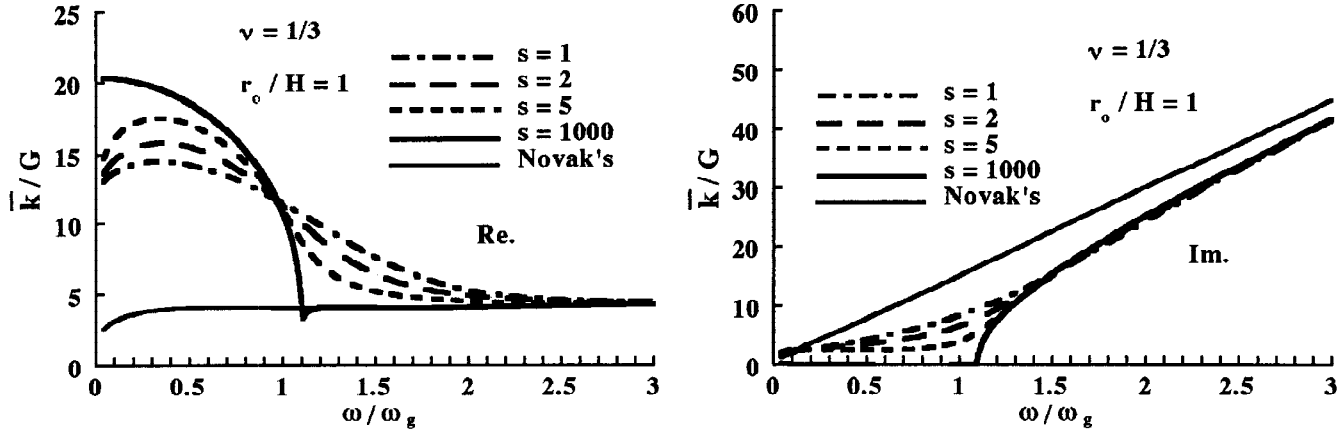

(a) Real parts of stiffness functions (b) Imaginary parts of stiffness functions

Fig. 3. Averaged horizontal stiffness functions of embedded rigid structures due to horizontal subgrade reactions of surrounding surface soil. (Poisson's ratio $\nu = 1/3$, $r_0 / H = 1$).

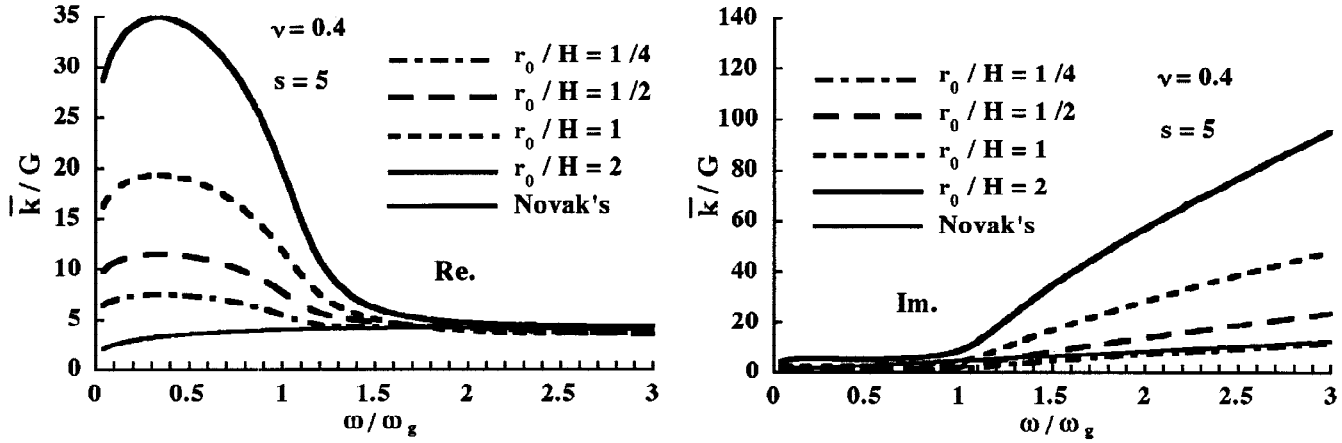

(a) Real parts of stiffness functions (b) Imaginary parts of stiffness functions

Fig. 4. Averaged horizontal stiffness functions of embedded rigid structures due to horizontal subgrade reactions of surrounding surface soil. (Poisson's ratio $\nu = 0.4$, impedance ratio $s = 5$).

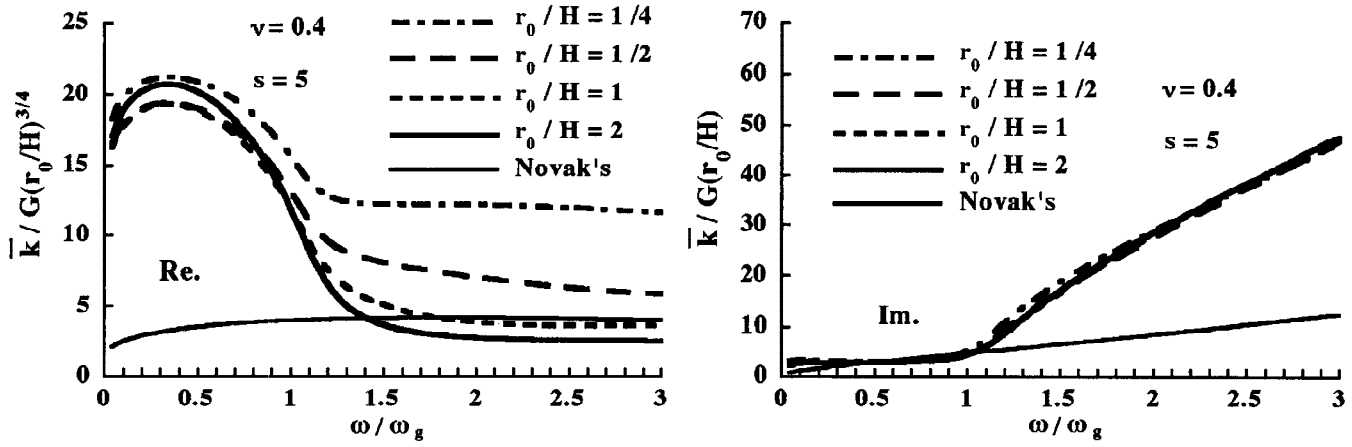

(a) Real parts of stiffness functions (b) Imaginary parts of stiffness functions

Fig. 5. Averaged horizontal stiffness functions of embedded rigid structures due to horizontal subgrade reactions of surrounding surface soil. (Poisson's ratio $\nu = 0.4$, impedance ratio $s = 5$).

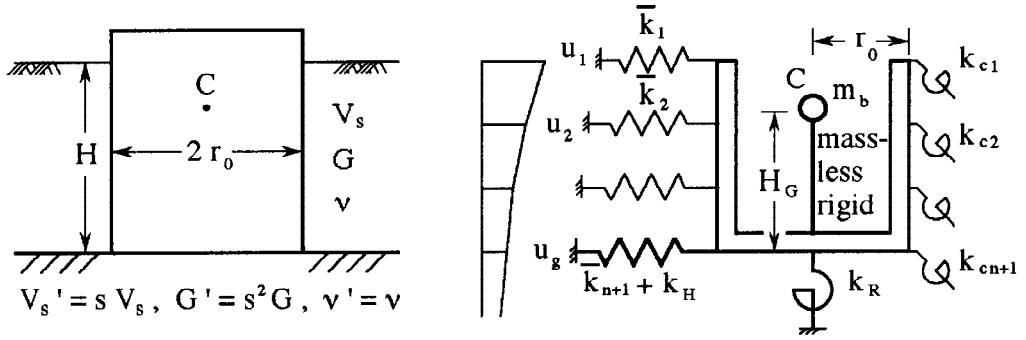

Fig. 6. A cylindrical rigid structure embedded in a finite soil stratum supported by a rock half-space.

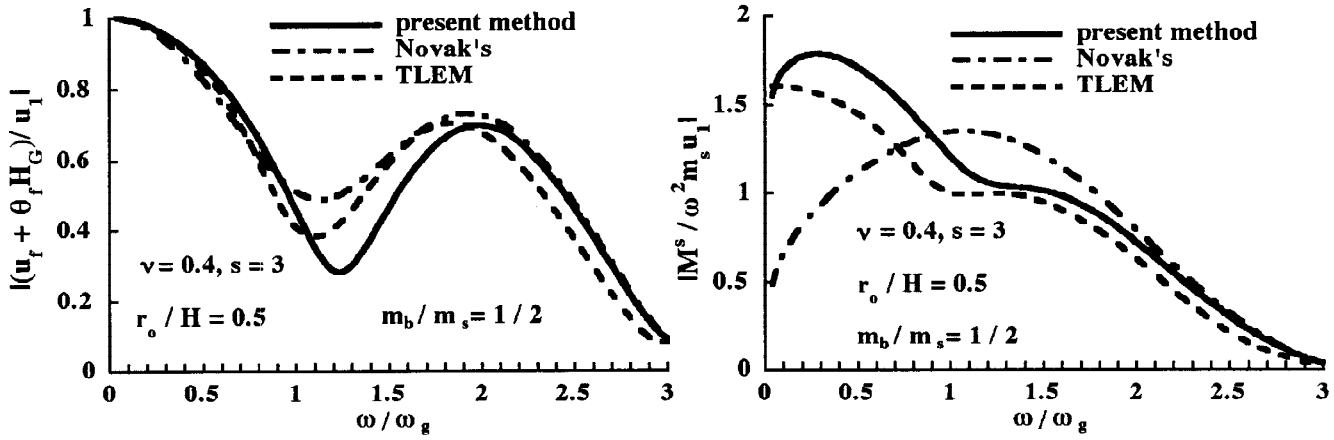

(a) Transfer functions, $|u_f+\theta_f H_G)/u_1|$ (b) Response functions, $|M^S/\omega^2 m_S u_1|$

Fig. 7. Transfer functions, $|u_f+\theta_f H_G)/u_1|$ and response functions of resultant moment of rigid structures, $|M^S/\omega^2 m_S u_1|$. (Poisson's ratio ν=0.4, s=3).

The validity of the proposed method was examined by comparing it to the results of the 3-dimensional thin approach. Results of the proposed method show good agreement with the 3-dimensional results, especially in the low frequency range. The proposed method in this paper can represent appropriate soil stiffnesses for embedded structures in a finite soil stratum on a rigid base or a rock half-space.

Acknowledgement

The authors wish to express their appreciation to Dr. H. Tajimi, Professor Emeritus of Nihon University, for his insightful suggestions and discussions.

REFERENCES

Ikeda, Y., Tajimi, H. and Shimomura, Y. (1992). A simplified method of obtaining interaction stiffnesses associated with the embedment of structures. *Proc. 10WCEE*, 1525-1530.

Novak, M., Nogami, T. and Aboul-Ella, F. (1978). Dynamic soil reactions for plane strain case. *Proc. ASCE, 104, No.EM4*, 953-959.

Shimomura, Y. and Ikeda, Y. (1995). A simplified seismic response analysis of an embedded structure. *Trans. 13SMiRT, III*, 79-84.

Tajimi, H., Minowa, C., and Shimomura, Y. (1977). Dynamic response of a large-scale shaking table foundation and its surrounding ground. *Proc. 7WECC, Vol.4*. 61-66.